Experimental and theoretical investigations of rate coefficients of the reaction S (3 P)+ O 2 in the temperature range 298–878 K

Chih-Wei Lu, Yu-Jong Wu, Yuan-Pern Lee, R. S. Zhu, and M. C. Lin

---

Articles you may be interested in

Experimental and theoretical investigation of rate coefficients of the reaction S (P 3) + OCS in the temperature range of 298 – 985 K
J. Chem. Phys. **125**, 164329 (2006); 10.1063/1.2357739

Experimental and theoretical studies of rate coefficients for the reaction O (P 3) + C H 3 O H at high temperatures
J. Chem. Phys. **122**, 244314 (2005); 10.1063/1.1924390

Determination of the internal state distribution of the SD product from the S (1 D)+ D 2 reaction
J. Chem. Phys. **122**, 024303 (2005); 10.1063/1.1827598

Isomers of OCS 2 : IR absorption spectra of OSCS and O(CS 2) in solid Ar
J. Chem. Phys. **121**, 12371 (2004); 10.1063/1.1822919

Rate coefficients for the reactions of Si (3 P J) with C 2 H 2 and C 2 H 4 : Experimental results down to 15 K
J. Chem. Phys. **115**, 6495 (2001); 10.1063/1.1396855

Experimental and theoretical investigations of rate coefficients of the reaction S(^{3}P)+O$_2$ in the temperature range 298–878 K

Chih-Wei Lu and Yu-Jong Wu
Department of Chemistry, National Tsing Hua University, Hsinchu 30013, Taiwan

Yuan-Pern Lee[a)]
Department of Chemistry, National Tsing Hua University, Hsinchu 30013, Taiwan and Institute of Atomic and Molecular Sciences, Academia Sinica, Taipei 10764, Taiwan

R. S. Zhu and M. C. Lin[b)]
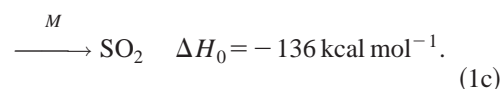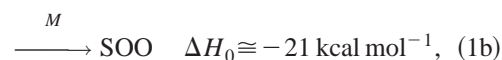*Department of Chemistry, Emory University, Atlanta, Georgia 30322*

Rate coefficients of the reaction S+O$_2$ with Ar under 50 Torr in the temperature range 298–878 K were determined with the laser photolysis technique. S atoms were generated by photolysis of OCS with a KrF excimer laser at 248 nm; their concentration was monitored via resonance fluorescence excited by atomic emission of S produced from microwave-discharged SO$_2$. Our measurements show that $k(298\text{ K})=(1.92\pm0.29)\times10^{-12}\text{ cm}^3\text{ molecule}^{-1}\text{ s}^{-1}$, in satisfactory agreement with previous reports. New data determined for 505–878 K show non-Arrhenius behavior; combining our results with data reported at high temperatures, we derive an expression $k(T)=(9.02\pm0.27)\times10^{-19}T^{2.11\pm0.15}\exp[(730\pm120)/T]\text{ cm}^3\text{ molecule}^{-1}\text{ s}^{-1}$ for $298\leqslant T\leqslant3460$ K. Theoretical calculations at the G2M (RCC2) level, using geometries optimized with the B3LYP/6-311+G(3df) method, yield energies of transition states and products relative to those of the reactants. Rate coefficients predicted with multichannel RRKM calculations agree satisfactorily with experimental observations; the reaction channel via SOO($^1A'$) dominates at $T<500$ K, whereas channels involving formation of SOO($^3A''$) followed by isomerization to SO$_2$ before dissociation, and formation of SOO($^1A''$) followed by direct dissociation, become important at high temperatures, accounting for the observed rapid increase in rate coefficient. © *2004 American Institute of Physics.* [DOI: 10.1063/1.1792611]

I. INTRODUCTION

The reaction of S(^{3}P) with O$_2$ is important in combustion chemistry; it plays an important role in the SO$_x$ emission during combustion of fuels containing sulfur compounds. Table I summarizes rate coefficients reported for this reaction. The rate coefficient for this reaction near room temperature has been extensively investigated and values are reported in the range $(1.5–2.8)\times10^{-12}\text{ cm}^3$ molecule^{-1} s^{-1}.[1–7] The temperature dependence of the rate coefficient below 423 K was reported to be small, with E_a/R values of 0 ± 50 K (Ref. 3) or $-(153\pm108)$ K.[6] Measurements of rate coefficients at high temperatures ($T\geqslant675$ K) have large discrepancies. Although the activation energy reported by Homann, Krome, and Wagner[8] ($E_a/R=2820$ K) is similar to that ($E_a/R=3110$ K) reported by Woiki and Roth,[9] the preexponential factors A vary more than fourfold. Saito *et al.*[10] reported a value $k=(6.3\pm1.2)\times10^{-12}\text{ cm}^3$ molecule^{-1} s^{-1} for temperatures between 1900 and 2200 K, about 0.4 times that reported by Woiki and Roth in this temperature range.[9] Matsui and co-workers[7,11] re-

ported $E_a/R=1840\pm300$ K for temperatures between 980 and 1610 K, much smaller than that reported by Woiki and Roth,[9] but rate coefficients determined in both works are within experimental uncertainties in the overlapping temperature range 1138–1610 K. No experimental data exist for temperatures between 423 and 980 K except much smaller, and likely erroneous, values reported by Homann, Krome, and Wagner for $T\geqslant675$ K.[8]

The reaction might proceed via various channels:

$$S(^3P)+O_2\rightarrow SO+O(^3P) \quad \Delta H_0=-5.5\text{ kcal mol}^{-1}, \tag{1a}$$

$$\xrightarrow{\;M\;} SOO \quad \Delta H_0\cong-21\text{ kcal mol}^{-1}, \tag{1b}$$

$$\xrightarrow{\;M\;} SO_2 \quad \Delta H_0=-136\text{ kcal mol}^{-1}. \tag{1c}$$

Formation of O atoms was observed near 300 K (Ref. 3) and at high temperatures.[9,10] Miyoshi *et al.*[7] reported the yield of O atom to be 1.05 ± 0.14 at 1566 K and 924 Torr, 1.06 ± 0.11 at 293 K and 2.02 Torr, and 1.04 ± 0.12 at 293 K and 50.2 Torr (all with Ar buffer gas), indicating that reactions (1b) and (1c) are unimportant.

The reaction of S(^{3}P) with O$_2$ is expected to proceed via multiple potential-energy surfaces (PES). Based on an ob-

---
a)Author to whom correspondence should be addressed. Electronic mail: yplee@mail.nctu.edu.tw
b)Author to whom correspondence should be addressed. Also at Center for Interdisciplinary Molecular Science, Chiao Tung University, Hsinchu, Taiwan. Electronic mail: chemmcl@emory.edu

TABLE I. Summary of reported experimental rate coefficients using various methods.

Temperature /K	Pressure (gas) /Torr	$k(\sim 298 \text{ K})$ /10^{-12},[a]	A /10^{-12},[a]	E_a/R /K	Method[b]	Author names	Reference
298	2.2 (Ar)	2.0 ±0.5			DF/CL	Fair and Thrush (FT)	1
298	60–200 (CO_2, Ar)	2.8 ±0.3			FP/ABS	Fair, Roodselaar, and Strausz (FRS)	2
295	113 (Ar)	1.7 ±0.3			FP/ABS	Donovan and Little (DL)	4
298	0.98–3.0 (He)	1.5 ±0.5			DF/RF	Clyne and Townsend (CT)	5
293	2–50 (Ar)	2.27±0.08			LP/LIF	Miyoshi *et al.* (MSTM)	7
252–423	20–200 (CO_2, He, Ar)	2.32±0.27	2.24±0.27	0±50	FP/RF	Davis, Klemm, and Pilling (DKP)	3
296–393	0.72–1.15 (Ar)	2.6 ±0.3	1.7±0.5	−(153±108)	DF/RF	Clyne and Whitefield (CW)	6
675–1090	1–60 (Ar)		16.6	2820	DF/MS	Homann, Krome, and Wagner (HKW)	8
980–1610	>578 (Ar)		25±6	1840±300	ST/ABS	Miyoshi *et al.* (MSTM)	7
1138–3463	281–953 (Ar)		69.8	3110	ST/ABS	Woiki and Roth (WR)	9
1900–2200	>1212 (Ar)		6.3±1.2[c]	0[c]	ST/ABS	Saito *et al.* (SUIKI)	10
298–878	50 (Ar)	1.92±0.29	[d]	[d]	LP/RF	This work	⋯

[a]In units of cm^3 molecule^{-1} s^{-1}.

[b]DF—discharge flow; FP—flash photolysis; LP—laser photolysis; ST—shock tube; CL—chemiluminescence; ABS—absorption; RF—resonance fluorescence; LIF—laser-induced fluorescence.

[c]$k(T) = 1.2 \times 10^{-13} T^{0.52}$ cm^3 molecule^{-1} s^{-1} for all data reported in the range 250–2200 K.

[d]$k(T) = (9.02 \pm 0.27) \times 10^{-19} T^{2.11 \pm 0.15} \exp[(730 \pm 120)/T]$ cm^3 molecule^{-1} s^{-1} for temperature range 298–3460 K.

served small rate coefficient, Fair *et al.* proposed that reaction (1) proceeds via SOO, which subsequently decomposes to SO+O;[2] the end-on attack to form SOO leads to an effective cross section for collisions much smaller than that associated with the side-on attack, hence a smaller rate coefficient. The existence of intermediate SOO is supported by its infrared absorption spectrum recorded after photolysis with laser radiation at 193 nm of an Ar matrix sample containing SO_2.[12] Craven and Murrell performed quasiclassical trajectory (QCT) calculations and predicted a rate coefficient of $(1.67 \pm 0.17) \times 10^{-12}$ cm^3 molecule^{-1} s^{-1} for reaction (1) at 298 K, in satisfactory agreement with experiment.[13,14] All trajectories show a common mechanism in which an initial SOO intermediate is formed, followed by rapid isomerization to OSO, which subsequently dissociates to O+SO. Lendvay, Shatz, and Harding performed a similar study with a many-body expansion (MBE) PES calibrated with extensive *ab initio* calculations.[15] Rodrigues and Varandas[16] performed QCT calculations with an accurate single-value double many-body expansion (DMBE) PES of SO_2 (Ref. 17) and obtained rate coefficients of reaction (1) and its reverse reaction in the temperature range 50–3500 K; the rate coefficient predicted at 300 K, $(6.21 \pm 0.08) \times 10^{-12}$ cm^3 molecule^{-1} s^{-1}, is about two to four times that determined experimentally. They indicate that nearly all trajectories evolve via intermediate SOO, and only about one quarter of the trajectories are associated with a long-lived SO_2 isomer having a lifetime ~ 1.5 ps.

We have performed careful experimental work on the reaction of $S+O_2$ under 50 Torr of Ar and extended rate measurements from 298 to 878 K to bridge between the region $T \leqslant 423$ K with a nearly temperature-independent rate coefficient and the region $T \geqslant 980$ K in which rate coefficients show an activation energy corresponding to $E_a/R = 1840–3110$ K. We also performed detailed theoretical cal-

culations to predict rate coefficients and to identify important channels in this reaction at various temperatures.

II. EXPERIMENTS

The experimental setup was described in detail previously;[18,19] only a brief description is given. The reaction vessel is a six-way tubular quartz cross (diameter 40 mm) with one axis having sidearms ≈ 15 cm in length and with Brewster windows for laser photolysis. The temperature of the reactor was regulated through resistive heating with a temperature controller (Omega CN 9000). S atoms were produced by photolysis of OCS with radiation from a pulsed KrF excimer laser at 248 nm (24–60 mJ cm^{-2}, 1–3 Hz). Excessive Ar gas was added to the system to ensure that most S(^{1}D) is quenched before reaction.[20] S atoms were excited with emission of S(^{3}S)–S(^{3}P$_{2,1,0}$) at 180.73, 182.03, and 182.62 nm, respectively, from a microwave-discharge lamp with a flowing gas mixture of $SO_2 \sim 0.10\%$ in He. An S1-UV lens (focal length $f = 5$ cm) served to collect light of wavelength $\lambda > 170$ nm and to discriminate against emission of shorter wavelength.

The fluorescence was collected perpendicular to both photolysis laser and probe beams with a MgF$_2$ lens ($f = 5$ cm) before being detected with a solar-blind photomultiplicr tube (EMR 541G-09). The signal was converted to voltage with a low-noise amplifier (Stanford Research Systems, SR570) before being transferred to a digital oscilloscope (Tektronix, TDS-620B, 2.5 GS s^{-1} with 500 MHz band width). The signal was typically averaged over more than 500 laser pulses. The temporal profiles of S atoms were transferred to a computer for further processing.

He (99.9995%), Ar (99.9995%), and O$_2$ (99.999%, all AGA Specialty Gases) were used without further purification. OCS (99.98%, Matheson) was purified through trap-to-

trap distillation. A 20% mixture of OCS in Ar was prepared with standard gas handling techniques. Flow rates of He, Ar, O$_2$, and the OCS/Ar mixture were monitored with mass flowmeters (Tylan FM360) that were calibrated with a wet testmeter and by the pressure increase in a calibrated volume before and after experiments.

Typical experimental conditions were as follows: total flow rate $F_T = 7 - 11$ STP cm^3 s^{-1} (STP=1 atm and 273 K), total pressure $P \cong 50$ Torr, reaction temperature $T = 298 - 878$ K, [OCS]$=(1.50 - 37.5) \times 10^{14}$ molecule cm^{-3}, [S]$=(1.4 - 33.4) \times 10^{11}$ molecule cm^{-3}, [O$_2$]$=(1.0 - 35.7) \times 10^{14}$ molecule cm^{-3}, [Ar]$=(5.5 - 16.5) \times 10^{17}$ molecule cm^{-3}, probed intervals of decay=20 μs–20 ms, and mean flow spced $v = 5.9 - 24.2$ cm s^{-1}.

III. COMPUTATIONAL METHODS

The geometries of reactants, intermediates, transition states, and products of the title reaction were optimized at the B3LYP/6-311+G($3df$) level of theory with Becke's three-parameter nonlocal exchange functional[21] and the nonlocal correlation functional of Lee, Yang, and Parr.[22] Energies of all species were calculated at the G2M(RCC2) level of theory[23] using geometries optimized with the B3LYP/6-311+G($3df$) method. Intrinsic reaction coordinate calculations[24] were performed to connect each transition state with designated reactants and products. All calculations were carried out with GAUSSIAN98 (Ref. 25) and MOLPRO 2002 programs.[26]

Rate coefficients for various reaction channels were calculated with a microcanonical variational RRKM method using the Variflex program.[27] The component rates were evaluated at E, J-resolved levels. The master equation was solved with an inversion approach for association and an eigenvalue-based approach for dissociation.[28,29] For the barrierless transition state, we used a Morse potential

$$E(R) = D_e[1 - e^{-\beta(R - R_e)}]^2, \quad (2)$$

in which D_e is the dissociation energy (D_0) plus zero-point energy, R_e is the equilibrium bond distance, and β is fitted from calculated potential energies at discrete atomic separations R, to represent the potential energy in a stretching mode along the minimum energy path of each individual reaction coordinate. In addition, a Lennard-Jones pairwise potential and an anisotropic potential (a form for potential anisotropy assuming a bonding potential that is cylindrically symmetric with respect to each fragment) are combined to form the final potential for calculation of the variational rate coefficient with the Variflex code. For tight transition states, numbers of states were calculated with the rigid-rotor harmonic-oscillator approximation.

IV. RESULTS AND DISCUSSION

A. Experimental rate coefficient

All experiments were carried out under pseudo-first-order conditions with [O$_2$]/[S] greater than 200. The initial concentration of S, [S]$_0$, was estimated from the absorption cross section (2.36×10^{-20} cm^2) of OCS and quantum yield $\Phi(S) = 0.72 \pm 0.08$ at 248 nm,[30] and the fluence of the pho-
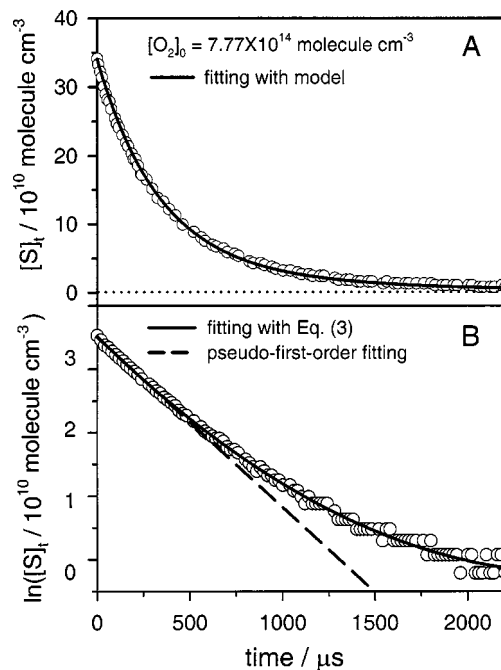

FIG. 1. (A) Temporal profiles of [S]$_t$ observed after photolysis of an Ar sample containing OCS and O$_2$. $T=878$ K, [O$_2$]$=7.77 \times 10^{14}$ molecule cm^{-3}, [OCS]$=3.83 \times 10^{14}$ molecule cm^{-3}, and [Ar] $=5.53 \times 10^{17}$ molecule cm^{-3}. The solid line represents fitted results according to a model described in the text. (B) Semilogarithmic plot of (A). The solid line represents fitted results according to Eq. (3) and the dashed line represents initial pseudo-first-order decay.

tolysis laser. Figure 1(a) shows a typical temporal profile of [S] observed when a flowing gas mixture containing OCS, O$_2$, and Ar was irradiated at 248 nm; a semilogarithmic plot is shown in Fig. 1(b). The relative concentration of S atoms, [S]$_t$, follows an exponential decay in the initial stage. The apparent pseudo-first-order rate coefficient k^1 may be derived with the equation

$$\ln([S]_t/[S]_0) = -k^1 t + at^2 - bt^3, \quad (3)$$

in which t is the reaction time and a and b are fitting parameters to account for secondary reactions. To derive accurate rate coefficients, we employed a model consisting of the following reactions:

$$S + O_2 \rightarrow SO + O \quad (1a)$$

$$\xrightarrow{M} SOO, \quad (1b)$$

$$SOO \xrightarrow{M} S + O_2 \quad (4a)$$

$$\xrightarrow{M} SO + O, \quad (4b)$$

$$S + OCS \rightarrow S_2 + CO, \quad (5)$$

$$O + SO \rightarrow S + O_2 \quad (6a)$$

$$\xrightarrow{M} SO_2, \quad (6b)$$

$$O + OCS \rightarrow S + CO_2 \tag{7a}$$

$$\rightarrow SO + CO, \tag{7b}$$

$$O + O_2 \xrightarrow{\quad M \quad} O_3, \tag{8}$$

$$SO + SO \rightarrow S + SO_2, \tag{9}$$

$$SO + O_2 \rightarrow O + SO_2, \tag{10}$$

$$S + SO_2 \rightarrow SO + SO, \tag{11}$$

$$O + S_2 \rightarrow SO + S, \tag{12}$$

for which rate coefficients have these reported dependences on temperature:

$$k_{1b}(T) = 1.09 \times 10^{-25} T^{-2.6}$$
$$\times \exp(-276/T) \ cm^6 \ molecule^{-2} \ s^{-1}, \tag{13}$$

$$k_{4a}(T) = 0.12 T^{-2.19}$$
$$\times \exp(-10630/T) \ cm^3 \ molecule^{-1} \ s^{-1}, \tag{14}$$

$$k_{4b}(T) = 7.02 \times 10^{-4} T^{-1.72}$$
$$\times \exp(-10803/T) \ cm^3 \ molecule^{-1} \ s^{-1}, \tag{15}$$

$$k_5(T) = 3.16 \times 10^{-19} T^{2.35}$$
$$\times \exp(-1253/T) \ cm^3 \ molecule^{-1} \ s^{-1} \tag{16}$$

$$k_{6a}(T) = 3.76 \times 10^{-18} T^{1.79}$$
$$\times \exp(-2230/T) \ cm^3 \ molecule^{-1} \ s^{-1} \tag{17}$$

$$k_{6b}(T) = 4.82 \times 10^{-31} (T/298)^{-2.17} \ cm^6 \ molecule^{-2} \ s^{-1} \tag{18}$$

$$k_{7a}(T) = 6.61 \times 10^{-11} \exp(-2706/T)$$
$$\times (0.4 - 202/T) \ cm^3 \ molecule^{-1} \ s^{-1} \ (Ref. \ 31) \tag{19}$$

$$k_{7b}(T) = 6.61 \times 10^{-11} \exp(-2706/T)$$
$$\times (0.6 + 202/T) \ cm^3 \ molecule^{-1} \ s^{-1} \ (Ref. \ 31) \tag{20}$$

$$k_8(T) = 2.16 \times 10^{-27} T^{-2.7} \ cm^6 \ molecule^{-2} \ s^{-1} \ (Ref. \ 32) \tag{21}$$

$$k_9(T) = 1.0 \times 10^{-12}$$
$$\times \exp(-1720/T) \ cm^3 \ molecule^{-1} \ s^{-1} \ (Ref. \ 33) \tag{22}$$

$$k_{10}(T) = 1.7 \times 10^{-12}$$
$$\times \exp(-4089/T) \ cm^3 \ molecule^{-1} \ s^{-1} \ (Ref. \ 34) \tag{23}$$

$$k_{11}(T) = 1.86 \times 10^{-40}$$
$$\times \exp(-4829/T) \ cm^3 \ molecule^{-1} \ s^{-1} \ (Ref. \ 35) \tag{24}$$
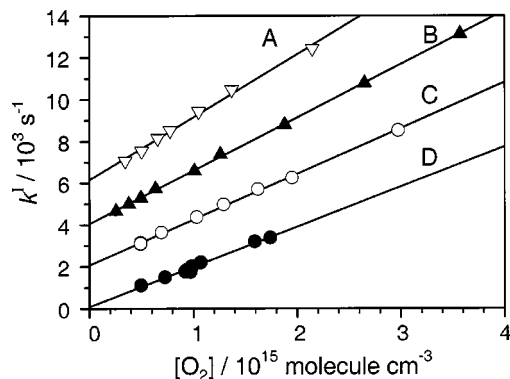

FIG. 2. Derived k_{1a}^I as a function of $[O_2]$ at various temperatures. (A) 878 K, symbol $\triangledown$; (B) 726 K, symbol $\blacktriangle$; (C) 658 K symbol $\bigcirc$; (D) 298 K symbol $\bullet$. The ordinates are shifted for each set of data for clarity.

$$k_{12}(T) = 2.2 \times 10^{-11}$$
$$\times \exp(-84/T) \ cm^3 \ molecule^{-1} \ s^{-1} \ (Ref. \ 14) \tag{25}$$

in which k_{1b}, k_{4a}, and k_{4b} are calculated results discussed in the following section, k_5 is derived on fitting data at high temperatures ($860 \leqslant T \leqslant 1680$ K) (Ref. 36) and low temperatures ($233 \leqslant T \leqslant 445$ K) (Ref. 37) to the equation, k_{6a} is derived on fitting data at high temperatures ($2212 \leqslant T \leqslant 3385$ K) (Ref. 38) and those at low temperatures ($252 \leqslant T \leqslant 423$ K) (Ref. 3) estimated from k_{1a} and the equilibrium constants based on ΔG of formation,[39] and k_{6b} is theoretically predicted in our previous work on pyrolysis of SO_2;[38] the latter agrees satisfactorily with the expression $9.3 \times 10^{-31} (T/298)^{-1.84} \ cm^6 \ molecule^{-2} \ s^{-1}$ reported by Grillo, Reed, and Slack.[40]

We modeled observed temporal profiles of $[S]_t$ with reactions (1a), (1b), and (4)–(12) with a commercial kinetic modeling program FACSIMILE;[41] rate coefficients listed in Eqs. (13)–(25) were held constant and the pseudo-first-order rate coefficient of the title reaction, k_{1a}^I, was varied to yield the best fit. Summary of experimental conditions and values of k_{1a}^I for 58 measurements in a temperature range 298–878 K may be found in Electronic Physics Auxiliary Publication Service (EPAPS); we list also k^I/k_{1a}^I for comparison.[42] Values of k^I obtained with Eq. (3) based on initial pseudo-first-order decays deviate from k_{1a}^I by less than 15% in most cases, indicating that secondary reactions play only a minor role under the initial experimental conditions. Detailed modeling shows that secondary reactions are negligible at low temperatures, whereas at high temperatures and with large $[OCS]$ and $[S]_0$ the corrections become greater; only reactions (5), (7a), and (7b) account for corrections greater than 3%.

Values of k_{1a}^I determined with various concentrations of O_2 at temperatures 298, 658, 726, and 878 K are plotted in Fig. 2, with ordinates shifted vertically for each line for clarity; the slope of the line fitted with least squares yields the bimolecular rate coefficient k_{1a} at each temperature. At 298 K, $k_{1a} = (1.92 \pm 0.08) \times 10^{-12} \ cm^3 \ molecule^{-1} \ s^{-1}$; unless otherwise noted, the uncertainty represents one standard error in fitting. In these experiments, rate coefficients remained

TABLE II. Bimolecular rate coefficients k_{1a} at various temperatures.

Temp /K	P /Torr	[S] $/10^{11,a}$	[O$_2$] $/10^{14,a}$	[Ar] $/10^{17,a}$	k_{1a} $/10^{-12,b}$
298	51	2.12–33.4	4.96–17.4	16.5	1.92±0.29
406	51	7.65	2.24–12.3	12.0	1.74±0.26
505	50	7.72	1.01–4.43	9.6	1.77±0.27
658	51	5.37–14.7	4.91–29.7	7.4	2.19±0.33
726	51	4.27	2.57–35.7	6.7	2.55±0.38
878	50	3.41–11.13	3.45–21.5	5.5	3.01±0.45

[a]In units of molecule cm^{-3}.
[b]In units of cm^3 molecule^{-1} s^{-1}.

the same while [S]$_0$ was varied from 2.1×10^{11} to 3.34×10^{12} molecule cm^{-3}. Combined systematic error (measurements of flow rates, pressure, and temperature) of our system is estimated to be ~8%, and the error in deriving k_{1a}^I and its dependence on [O$_2$] is ~12%. Hence, we estimate an error ~15% for k_{1a} and recommend a rate coefficient $(1.92 \pm 0.29) \times 10^{-12}$ cm^3 molecule^{-1} s^{-1} at 298 K.

    Rate coefficients k_{1a} determined at 298, 406, 505, 658, 726, and 878 K are listed in Table II. k_{1a} remains approximately constant from 298 to 505 K, but increases from ~1.8×10^{-12} to 3.0×10^{-12} cm^3 molecule^{-1} s^{-1} as the temperature increases further to 878 K. In the temperature range 298–505 K, rate coefficients show a small negative temperature dependence with $E_a/R = -(65 \pm 40)$ K. Reported rate coefficients are compared in Table I and Fig. 3; lines of various types are drawn for only the range of temperature investigated. The value of k_{1a} at 298 K determined in this work is within experimental uncertainties of previous reports by Fair and Thrush (designated FT in Fig. 3),[1] Donovan and Little (DL),[4] Clyne and Townsend (CT),[5] Miyoshi *et al.* (MSTM),[7] and Davis, Klemm, and Pilling (DKP),[3] but is slightly smaller than values of $(2.6 \pm 0.3) \times 10^{-12}$ cm^3 molecule^{-1} s^{-1} by Clyne and Whitefield (CW)[6] and $(2.8 \pm 0.3) \times 10^{-12}$ cm^3 molecule^{-1} s^{-1} by Fair, Roodselaar, and Strausz (FRS).[2] The small negative activation energy of $E_a/R = -(65 \pm 40)$ K is consistent also with two previous reports of $E_a/R = -(153 \pm 108)$ K by CW[6] and 0 ± 50 K by DKP,[3] even though their rate coefficients are slightly greater
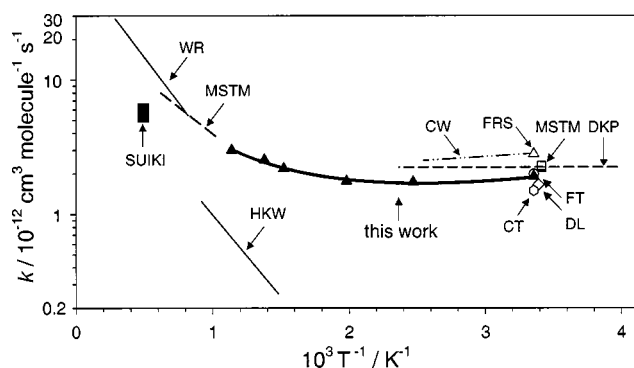
FIG. 3. Arrhenius plots of k_{1a} for the reaction S+O$_2$→O+SO. Our data are shown as symbols ▲ with a fitted equation shown as a thick solid line. Previous results on temperature dependence are shown as lines of various types drawn for the temperature range of study. A combination of first characters of each authors last name is used to indicate previous reports, as listed in Table I.
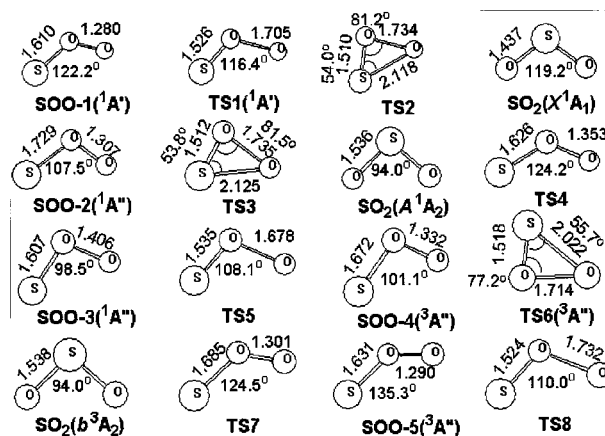
FIG. 4. Optimized geometries of transition states and intermediates of the S+O$_2$ system at the B3LYP/6-311+G($3df$) level, with bond lengths in Å and bond angles in degree. Small and large solid spheres in the structures represent O and S atoms, respectively.

than ours. Rate coefficients at 505–878 K are new; they match well with rate coefficients reported for $T \geq 980$ K by MSTM (Ref. 7) and WR,[9] as illustrated in Fig. 3.

    Fitting our results yields an expression for the rate coefficient in the range $298 \leq T \leq 878$ K:

$$k_{1a}(T) = (8.60 \pm 0.34) \times 10^{-20} T^{2.40 \pm 0.24}$$
$$\times \exp[(960 \pm 120)/T] \ \text{cm}^3 \ \text{molecule}^{-1} \ \text{s}^{-1}.$$

(26)

When combined with data at high temperatures by MSTM and WR, a general expression

$$k_{1a}(T) = (9.02 \pm 0.27) \times 10^{-19} T^{2.11 \pm 0.15}$$
$$\times \exp[(730 \pm 120)/T] \ \text{cm}^3 \ \text{molecule}^{-1} \ \text{s}^{-1}$$

(27)

is derived for $298 \leq T \leq 3460$ K. This equation reproduces reported rate coefficients by MSTM, WR, and our work to within 30% except a few data points.

B. Potential-energy surfaces and reaction mechanism

    Our calculations show that several triplet and singlet intermediates and transition states are involved in the reaction S(^{3}P)+O$_2$($X\,^3\Sigma_g^-$) to produce SO($X\,^3\Sigma^-$)+O(^{3}P). Optimized geometries of the intermediates and transition states involved in the reaction are shown in Fig. 4. The energy diagrams for singlet and triplet surfaces calculated with the G2M(RCC2)//B3LYP/6-311+G($3df$) method are presented in Fig. 5. Predicted vibrational wave numbers and rotational constants as well as available experimental data[43–47] for the species involved are discussed and summarized in Table 4 of Ref. 38. The results indicate that the predicted vibrational wave numbers are underestimated by 0.2%–2.3% from experimental values.

    The predicted enthalpy of reaction, -4.8 kcal mol^{-1}, for reaction (1a) is near the value obtained from JANAF Thermalchemical Tables, -5.5 kcal mol^{-1}.[39] Figure 5 shows that S(^{3}P)+O$_2$($X\,^3\Sigma_g^-$) might proceed via singlet and triplet SOO intermediates. The singlet channels involve two sur-
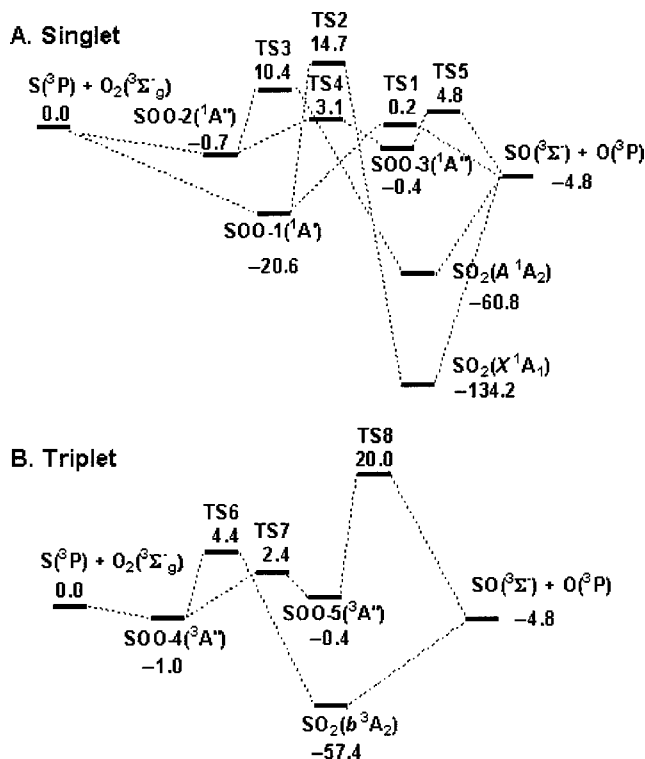
FIG. 5. Potential-energy diagrams for the $S+O_2$ reaction based on energies calculated at the G2M(RCC2)//B3LYP/6-311+G(3df) level: (A) singlet system and (B) triplet system. Energies are listed in kcal mol^{-1}.

faces, $^1A'$ and $^1A''$. The $^1A'$ intermediate (SOO-1) is more stable than those of $^1A''$ (SOO-2 and SOO-3) and has no barrier for formation from $S(^3P)+O_2(X\,^3\Sigma_g^-)$. The predicted energy of SOO-1, 113.6 kcal mol^{-1} above $SO_2(X\,^1A_1)$, is similar to a value of 117 kcal mol^{-1} predicted by Kellogg and Schaefer,[48] but greater than a value of 105 kcal mol^{-1} predicted by Dunning and Raffenetti[49] who employed a two-reference CI method with generalized valence-bond (GVB) natural orbitals. SOO-1 can directly dissociate to SO+O via TS1 lying only about 0.2 kcal mol^{-1} above $S(^3P)+O_2(X\,^3\Sigma_g^-)$. This channel is hence the most important path at low temperature. Otherwise, SOO-1 can isomerize to $SO_2(X\,^1A_1)$ via TS2 with a large barrier, 14.7 kcal mol^{-1} above the reactants; this process is kinetically unimportant for the formation of SO+O. The second singlet channel proceeds via SOO-2($^1A''$) and SOO-3($^1A''$) to form SO+O. TS4 connects SOO-2($^1A''$) and SOO-3($^1A''$), and TS5 corresponds to dissociation of SOO-3($^1A''$) to the products. Transition states TS4 and TS5 lie 3.1 and 4.8 kcal mol^{-1}, respectively, above $S+O_2$. In addition, SOO-2 can isomerize to $SO_2(A\,^1A_2)$ via TS3 with a barrier of 10.4 kcal mol^{-1} above the reactants, followed by dissociation to products.

The triplet channel proceeds via SOO-4($^3A''$) without a barrier, followed by formation of $SO_2(b\,^3A_2)$ and SOO-5($^3A''$) via TS6 and TS7 with barriers of 5.4 and 3.4 kcal mol^{-1}, respectively. $SO_2(b\,^3A_2)$ directly dissociates to SO+O with an endothermicity of 52.6 kcal mol^{-1} and SOO-5($^3A''$) dissociates to SO+O via TS8 at 20.0 kcal mol^{-1} above $S(^3P)+O_2(X\,^3\Sigma_g^-)$. The above singlet

channel via TS4 and TS5 and the triplet channel via TS6 are expected to be insignificant at low temperatures, but become important at high temperatures.

The quintuplet surface is also investigated in this work, but no stable intermediates are found. One direct abstraction channel with a linear transition state is located; it lies 54.4 kcal mol^{-1} above the reactants $S+O_2$. Hence, the contribution of quintuplet surfaces to production of SO+O is negligible even at high temperature.

Calculations based on variational transition-state and RRKM theories were carried out with the Variflex code[27] for the overall reaction

$$S+O_2 \rightarrow SO+O \tag{1a}$$

via three possible channels to yield rate coefficients

$$k_{1a\text{-}1}(T)=6.78\times10^{-14}T^{0.53}$$
$$\times\exp(-15/T)\ \text{cm}^3\ \text{molecule}^{-1}\ \text{s}^{-1}, \tag{28}$$

$$k_{1a\text{-}2}(T)=1.07\times10^{-14}T^{0.96}$$
$$\times\exp(-1980/T)\ \text{cm}^3\ \text{molecule}^{-1}\ \text{s}^{-1}, \tag{29}$$

$$k_{1a\text{-}3}(T)=8.69\times10^{-15}T^{0.89}$$
$$\times\exp(-2240/T)\ \text{cm}^3\ \text{molecule}^{-1}\ \text{s}^{-1}. \tag{30}$$

Channel 1 proceeds via SOO-1($^1A'$) and TS1 that has the smallest barrier relative to $S+O_2$. Channel 2 involves SOO-4($^3A''$) and TS6 on the triplet surface, with an energy of 4.4 kcal mol^{-1}, whereas channel 3 proceeding via SOO-2($^1A''$), TS4, SOO-3($^1A''$), and TS5; TS5 has the greatest energy (4.8 kcal mol^{-1}) among these three channels. The predicted total rate coefficients are expressed as

$$k_{1a}(T)=1.29\times10^{-17}T^{1.78}$$
$$\times\exp(430/T)\ \text{cm}^3\ \text{molecule}^{-1}\ \text{s}^{-1}. \tag{31}$$

In the above calculations, the association from $S+O_2$ to the potential minimum SOO-1($^1A'$) was calculated on increasing the S-O bond distance from its equilibrium value of 1.610 to 3.740 Å at intervals of 0.1 Å with the B3LYP/6-311+G(3df) method; the calculated energies were fitted to a Morse equation [Eq. (2)] to evaluate β=4.06 Å^{-1}. For the associations from $S+O_2$ to SOO-2($^1A''$) and to SOO-4($^3A''$), because the wells are shallow, -0.7 and -1.0 kcal mol^{-1}, the rate coefficients for channels 2 and 3 are controlled by tight transition states TS4 and TS6, respectively; furthermore, because structures of SOO-1($^1A'$), SOO-2($^1A''$), and SOO-4($^3A''$) are similar, the same value of β (4.06 Å^{-1}) was used for the association processes. Dissociation energics predicted at the G2M level are used in calculations of the rate coefficient for association. The Lennard-Jones (LJ) parameters required for the RRKM calculations are the same as those used for the reaction O+SO previously.[38] The exponential-down model with α=1500 cm^{-1} is employed for collisional deactivation. Because the electronic ground state of the S atom is split into three (quintuplet, triplet, and singlet) degenerate levels separated by 396.1 and 573.6 cm^{-1}, the electronic partition function of these low-lying excited states are also taken into account in calculations of the rate constant.
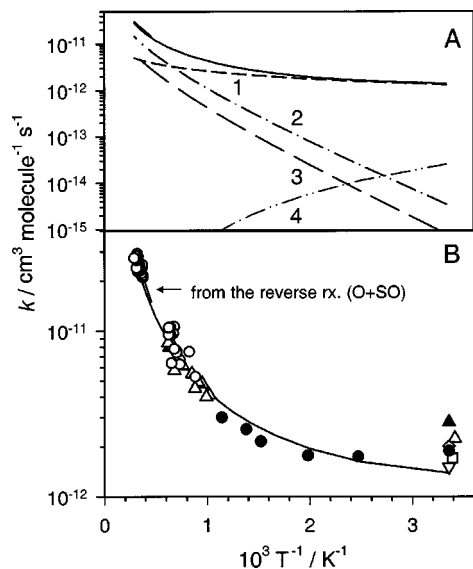
FIG. 6. (A) Theoretically predicted rate coefficients for the reaction S $+$O$_2\rightarrow$O$+$SO. Channel 1—via SOO-1($^1A'$) and TS1; channel 2—via SOO-4($^3A''$), TS6, and SO$_2$($b\,^3A_2$); channel 3—via SOO-2($^1A''$), TS3, SOO-3($^1A''$), and TS4; channel 4—rate of association of SOO($^1A'$); solid line—total rate coefficient. (B) Comparison of predicted total rate coefficient k_{1a} (solid line) with experimental data (●—this work; ○—Woiki and Roth (Ref. 9); △—Miyoshi *et al.* (Ref. 7); ◇—Fair and Thrush (Ref. 1); ▲: Fair, Roodselaar, and Strausz (Ref. 2); ▽—Clyne and Townsend (Ref. 5); □—Donovan and Little (Ref. 4).

Rate coefficients for each channel and the total rate coefficient, Eq. (31), for the title reaction are plotted in Fig. 6(a); the total rate coefficient is compared with experimental results on an expanded scale in Fig. 6(b). Channel 1 is clearly the only available path at temperatures below 500 K, whereas channels 2 and 3 become important at higher temperatures, resulting in a more rapid increase of the rate coefficient at high temperatures. The total rate coefficient agrees satisfactorily with experimental results in this work, and also with those at high temperatures reported by Miyoshi *et al.*[7] and by Woiki and Roth.[9] In our previous experiments using a diaphragmless shock tube to investigate pyrolysis of SO$_2$,[38] we observed formation of S atoms from the secondary reaction,

$$O+SO\rightarrow S+O_2, \tag{6a}$$

and determined a rate coefficient for the temperature range 2212–3385 K

$$k_{6a}(T)=(3.0\pm0.3)\times10^{-11}$$
$$\times\exp[-(6980\pm280)/T]\ \text{cm}^3\,\text{molecule}^{-1}\,\text{s}^{-1}. \tag{32}$$

Combining with the equilibrium constant derived from literature values of $\Delta G(T)$ for the corresponding species,[39] we derive the rate expression for the title reaction in the temperature range 2212–3385 K to be

$$k_{1a}(T)=(1.1\pm0.3)\times10^{-11}$$
$$\times\exp[-(4360\pm220)/T]\ \text{cm}^3\,\text{molecule}^{-1}\,\text{s}^{-1}. \tag{33}$$

The results are consistent with previous experimental results by Woiki and Roth,[9] and our theoretical predictions described above, as compared in Fig. 6.

The formation of SO$_2$ via channel 2 is negligibly small. SOO might be produced at high pressure and low temperature via channel 1 [Reaction (1b)]; subsequent decomposition might produce S$+$O$_2$ and SO$+$O:

$$\text{SOO-1}(^1A')\xrightarrow{M} S+O_2, \tag{4a}$$

$$\xrightarrow{M} SO+O. \tag{4b}$$
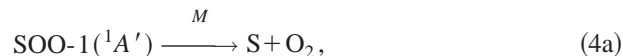
Rate coefficients for reactions (1b), (4a), and (4b) are predicted, as listed in Eqs. (13)–(15); they are negligibly small at 50 Torr and 298 K.

It must be mentioned that the predicted rate coefficients at low temperatures are sensitive to pressure and the energy of TS1. Our results show that, at 298 K, increasing the pressure to 700 Torr and decreasing the exit barrier of TS1 by 0.2 kcal mol^{-1} can well reproduce the experimental value; a negative temperature-dependent effect on the rate coefficient k_{1a} in the low temperature range, 200–298 K, is also obtained, which is attributed to combined effects of the barrierless association reaction (1b) and the decomposition reaction (4b).

V. CONCLUSION

Rate coefficients for the reaction of S with O$_2$ to form O and SO in the temperature range 298–878 K are determined using laser photolysis for production of S atoms and resonance fluorescence for detection of S atoms. Our result at 298 K, $k_{1a}=(1.92\pm0.29)\times10^{-12}$ cm^3 molecule^{-1} s^{-1}, is consistent with previous measurements, and new data in the range 505–878 K fill the gap between reported rate coefficients for $T\leqslant423$ K and $T\geqslant980$ K. From combined available data, rate coefficients fit well with the equation $k_{1a}(T)=(9.02\pm0.27)\times10^{-19}T^{2.11\pm0.15}\exp[(730\pm120)/T]$ cm^{3}molecule^{-1} s^{-1} for temperatures in the range 298–3460 K; listed uncertainties represent one standard error in fitting. Theoretical calculations based on PES computed at the G2M(RCC2)//B3LYP/6-311$+(3df)$ level indicate that the reaction proceeds to form SOO having various conformations; the reaction path via SOO($^1A'$) to form SO$+$O dominates at $T\leqslant500$ K, but two additional paths, one via SOO($^3A''$) then SO$_2$ and one via SOO($^1A'$), become important at high temperatures. Predicted total rate coefficients agree with experiments throughout the temperature range under investigation. Predicted and reported experimental rate coefficients at high temperatures also agree satisfactorily with those calculated based on the reverse reaction O$+$SO and equilibrium constants.

ACKNOWLEDGMENTS

[1] R. W. Fair and B. A. Thrush, Trans. Faraday Soc. **65**, 1557 (1969).

[2] R. W. Fair, A. van Roodselaar, and O. P. Strausz, Can. J. Chem. **49**, 1659 (1971).

[3] D. D. Davis, R. B. Klemm, and M. Pilling, Int. J. Chem. Kinet. **4**, 367 (1972).

[4] R. J. Donovan and D. J. Little, Chem. Phys. Lett. **13**, 488 (1972).

[5] M. A. A. Clyne and L. W. Townsend, Int. J. Chem. Kinet. **1**, 73 (1976).

[6] M. A. A. Clyne and P. D. Whitefield, J. Chem. Soc., Faraday Trans. 2 **75**, 1327 (1979).

[7] A. Miyoshi, H. Shiina, K. Tsuchiya, and H. Matsui, Symp. Int. Combust. Proc. **26**, 535 (1996).

[8] K. H. Homann, G. Krome, and H. Gg. Wagner, Ber. Bunsenges. Phys. Chem. **72**, 998 (1968).

[9] D. Woiki and P. Roth, Int. J. Chem. Kinet. **27**, 59 (1995).

[10] K. Saito, Y. Ueda, R. Ito, T. Kakumoto, and A. Imamura, Int. J. Chem. Kinet. **18**, 871 (1986).

[11] K. Tsuchiya, K. Kamiya, and H. Matsui, Int. J. Chem. Kinet. **29**, 57 (1997).

[12] L.-S. Chen, C.-I. Lee, and Y.-P. Lee, J. Chem. Phys. **105**, 9454 (1996).

[13] J. N. Murrell, W. Craven, and S. C. Farantos, Mol. Phys. **49**, 1077 (1983).

[14] W. Craven and J. N. Murrell, J. Chem. Soc., Faraday Trans. 2 **83**, 1733 (1987).

[15] G. Lendvay, G. C. Shatz, and L. B. Harding, Faraday Discuss. **102**, 389 (1995).

[16] S. P. J. Rodrigues and A. J. C. Varandas, J. Phys. Chem. A **107**, 5369 (2003).

[17] A. J. C. Varandas and S. P. J. Rodrigues, Spectrochim. Acta, Part A **58**, 629 (2002).

[18] E. W.-G. Diau and Y.-P. Lee, J. Chem. Phys. **96**, 377 (1992).

[19] L.-H. Lai, Y.-C. Hsu, and Y.-P. Lee, J. Chem. Phys. **97**, 3092 (1992).

[20] G. Blake and L. E. Jusinski, J. Chem. Phys. **82**, 789 (1985).

[21] A. D. Becke, J. Chem. Phys. **98**, 5648 (1993); *ibid.* **96**, 2155 (1992); *ibid.* **97**, 9173 (1992).

[22] C. Lee, W. Yang, and R. G. Parr, Phys. Rev. B **37**, 785 (1988).

[23] A. M. Mebel, K. Morokuma, and M. C. Lin, J. Chem. Phys. **103**, 7414 (1995).

[24] C. Gonzalez and H. B. Schlegel, J. Phys. Chem. **90**, 2154 (1989).

[25] M. J. Frisch, G. W. Trucks, H. B. Schlegel *et al.*, GAUSSIAN 98, Revision A.9, Gaussian Inc., Pittsburgh, PA, 1998.

[26] MOLPRO is a package of *ab initio* programs written by H.-J. Werner and P. J. Knowles, with contributions from J. Almlöf, R. D. Amos, A. Berning *et al.*

[27] S. J. Klippenstein, A. F. Wagner, R. C. Dunbar, D. M. Wardlaw, and S. H. Robertson, VARIFLEX: Version 1.00, 1999.

[28] R. G. Gilbert and S. C. Smith, *Theory of Unimolecular and Recombination Reactions* (Blackwell Scientific, Carlton, Australia, 1990).

[29] K. A. Holbrook, K. J. Pilling, and S. H. Robertson, *Unimolecular Reactions* (Wiley, Chichester, U.K., 1996).

[30] R. N. Rudolph and E. C. Y. Inn, J. Geophys. Res., C: Oceans Atmos. **86**, 9891 (1981).

[31] N. Isshiki, Y. Murakami, K. Tsuchiya, A. Tezaki, and H. Matsui, J. Phys. Chem. A **107**, 2464 (2003).

[32] H. Hippler, R. Rahn, and J. Troe, J. Chem. Phys. **93**, 6560 (1990).

[33] K. Schofield, Combust. Flame **124**, 137 (2001).

[34] K. Tsuchiya, K. Kamiya, and H. Matsui, Int. J. Chem. Kinet. **29**, 57 (1997).

[35] Y. Murakami, S. Onishi, T. Kobayashi, N. Fujii, N. Isshiki, K. Tsuchiya, A. Tezaki, and H. Matsui, J. Phys. Chem. A **107**, 10996 (2003).

[36] H. Shiina, M. Oya, K. Yamashita, A. Miyoshi, and H. Matsui, J. Phys. Chem. **100**, 2136 (1996).

[37] R. B. Klemm and D. D. Davis, J. Phys. Chem. **78**, 1137 (1974).

[38] C.-W. Lu, Y.-J. Wu, Y.-P. Lee, R. S. Zhu, and M. C. Lin, J. Phys. Chem. A **107**, 11020 (2003).

[39] M. W. Chase, Jr., J. Phys. Chem. Ref. Data Monogr. **9**, 1 (1998).

[40] A. Grillo, R. Reed, and M. W. Slack, J. Chem. Phys. **70**, 1634 (1979).

[41] FACSIMILE is a computer software for modeling process and chemical-reaction kinetics released by AEA Technology, Oxfordshire, United Kingdom.

[42] See EPAPS Document No. E-JCPSA6-121-027438 for experimental conditions and values of K^I_{1a}. A direct link to this document may be found in the online article's HTML reference section. The document may also be reached via the EPAPS homepage (http://www.aip.org/pubservs/epaps.html) or from ftp.aip.org in the directory /epaps/. See the EPAPS homepage for more information.

[43] T. Shimanouchi, *Tables of Molecular Vibrational Frequencies Consolidated* (National Bureau of Standards, Gaithersberg, MD, 1972), Vol. 1, pp. 1–160.

[44] A. G. Hopkins and C. W. Brown, J. Chem. Phys. **62**, 2511 (1975).

[45] C.-C. Zen, I.-C. Chen, and Y.-P. Lee, J. Phys. Chem. A **104**, 771 (2000).

[46] C. L. Huang, I.-C. Chen, A. J. Merer, C.-K. Ni, and A. H. Kung, J. Chem. Phys. **114**, 1187 (2001).

[47] L.-S. Chen, C.-I. Lee, and Y.-P. Lee, J. Chem. Phys. **105**, 9454 (1996).

[48] C. B. Kellogg and H. F. Schaefer III, J. Chem. Phys. **102**, 4177 (1995).

[49] T. H. Dunning and R. C. Raffenetti, J. Am. Chem. Soc. **85**, 1350 (1981).